Cyy-287, a novel pyrimidine-2,4-diamine derivative, efficiently mitigates inflammatory responses, fibrosis and lipid synthesis in obesity-induced cardiac and hepatic dysfunction

Jinhuan Ni[1], Xiaodan Zhang[1], Huijing Huang[1], Zefeng Ni[2], Jianchao Luo[1], Yunshan Zhong[1],

Min Hui[1], Zhiguo Liu[2,*], Jianchang Qian[1,*], Qianwen Zhang[1,*]

1 Institute of Molecular Toxicology and Pharmacology, Wenzhou Medical University, Wenzhou 325035, China

2 Chemical Biology Research Center at School of Pharmaceutical Sciences, Wenzhou Medical University, Wenzhou 325035, China

Corresponding Author:

Zhiguo Liu, Ph.D, Professor

Chemical Biology Research Center at School of Pharmaceutical Sciences, Wenzhou Medical University, Wenzhou 325035,China

Email address: lzgcnu@163.com

Jianchang Qian, Ph.D, Professor

Institute of Molecular Toxicology and Pharmacology, Wenzhou Medical University, Wenzhou 325035, China

Email address: qianjc@wmu.edu.cn

Qianwen Zhang, Ph.D

Institute of Molecular Toxicology and Pharmacology, Wenzhou Medical University, Wenzhou 325035, China

Email address: zqwlovelove@126.com

Abstract

Background. Inflammation and metabolic disorder caused by obesity are important factors leading to the occurrence and development of obesity complications. In the present study, we investigated the protective effect and underlying mechanism of a novel pyrimidine-2,4-diamine derivative, cyy-287, in high-fat diet (HFD) mice.

Methods. Based on their diets for 10 weeks, the mice were categorized into the following four groups ($n \geq 7$): control (regular diet), HFD, HFD with Cyy-287 (5 mg/kg), HFD with Cyy-287 (20 mg/kg) for 10 weeks. Echocardiography revealed the parameters of diastolic function of the heart. Hematoxylin and eosin (HE) staining of the sections revealed hepatic steatosis.

Results. Cyy-287 administration increased ejection fraction (EF) and fractional shortening (FS) index and decreased the the levels of serum glucose and lipid markers and transaminase activities in HFD mice. Furthermore, Cyy-287 inhibited the histopathological changes in the heart and liver and decreased inflammatory activity. Significantly, Cyy-287 diminished p38 mitogen-activated protein kinase (MAPK), the nuclear factor-kappa B (NF-κB) axis and sterol regulatory element-binding protein-1c (SREBP-1c), as well as upregulated the AMP-activated protein kinase (AMPK) pathway, in HFD mice.

Conclusions. These findings suggest that that Cyy-287 protected heart and liver cells from obesity-induced damage by inhibiting inflammation, fibrosis and lipid synthesis.

Keyword: Cyy-287, inflammation, obesity complications, p38, AMPK

Introduction

Obesity is a common public health problem that is often accompanied by a variety of complications, such as cardiovascular and cerebrovascular diseases, nephropathy, diabetes, and fatty liver (*Caballero, 2019; Polyzos, Kountouras & Mantzoros, 2019; Piche, Tchernof & Despres, 2020*). All these complications pose a serious threat to the health of obese patients and reduce their quality of life. Although weight controlling can alleviate its progression, drug treatment is still one of the most efficiency ways to alleviate the development of obesity complications (*Jackson et al., 2015; Narayanaswami & Dwoskin, 2017; Srivastava & Apovian, 2018*). At present, the basic treatment strategies include blood pressure reduction, lipid reduction, hypoglycemic, and so on (*Tanaka, 2020; Klop & Elte, 2013*). However, these treatments cannot block the progression of the disease completely. Therefore, it is necessary to determine new therapeutic strategies and develop new therapeutic drugs.

Chronic inflammation, intracellular mitochondrial dysfunction, insulin resistance, metabolic disorders, autophagy, and endoplasmic reticulum stress are important mechanisms that induce obesity complications (*Ye, 2021; Fu et al., 2011; Goldman S, Zhang & Jin S, 2010; Aron-Wisnewsky et al., 2020*). Among them, the inflammatory response is a crucial process in the development of tandem pathologym (*Cox AJ, West & Cripps., 2015*). Nuclear factor-κB (NF-κB) regulates a large number of genes involved in different processes of the immunomodulatory responses. The mechanism of NF-κB activation is the inducible degradation of IκBα triggered through its site-specific phosphorylation by a multi-subunit IκB kinase (IKK) complex. IKK can be activated by various factors, including cytokines, growth factors, mitogens, and stress agents (*Nguyen & Stamper, 2017)*. Recently, it has been suggested that sporoderm-broken spore of Ganoderma lucidum (BSGLP) can inhibit the upregulation of the NF-κB signaling pathway in adipose tissue induced by high-fat diet (HFD), thus suppressing obesity and hyperlipidemia by modulating inflammation, gut microbiota, and intestinal tract barrier function (*Sang., 2020)*. Another study has confirmed that controlling adipose inflammation mediated by adipose tissue macrophages can improve metabolic dysfunction and reduce obesity (*Wu, Shi & Wang, 2021*). Consequently, blocking inflammatory response by targeting NF-κB pathway may be an effective way against obesity complications.

AMP-activated protein kinased (AMPK), a serine/threonine protein kinase, senses cellular energy status and is activated by higher AMP/ATP or ADP/ATP ratios (*Lv et al., 2019*).

80   Its functions extend to various pathways, including those linked to metabolic diseases (*Fogarty*

81   *et al, 2016*). Emerging evidence shows that AMPK activation is beneficial for the treatment of

82   several metabolic diseases, including obesity and nonalcoholic fatty liver disease (NAFLD)

83   (*Garcia et al., 2019*). And several natural compounds and synthetic drugs have been recognized

84   to prevent obesity-related renal injury, cardiomyopathy, and hepatic damage by activating

85   AMPK and its downstream pathways (*Li et al., 2021; Li et al;2022*). In addition, AMPK

86   activation can effectively prevent inflammation induced hepatic steatosis though the IKK/NF-κB

87   signaling pathway (*Li et al., 2018; Jiang et al., 2021*). Based on these studies, we speculate that

88   targeting AMPK pathway could represent a new potential strategy for obesity complications.

89   Previously, we investigated the antitumor effect and underlying mechanism of a novel

90   pyrimidine-2,4-diamine derivative, Cyy-287 (**Fig. 1A**), in non-small cell lung cancer (*Zhang et*

91   *al., 2022*). Due to the fact that C57BL/6J mice exhibited comparable phenotypes to those found

92   in human diabetes and metabolic disorders following a high-fat diet, we developed a mouse

93   model of high-fat diet-induced obesity using C57BL/6J mice. We found that the differential

94   genes between the control group and the cyy-287 group were enriched in the inflammatory

95   pathway. In present study, our data suggested that Cyy-287 could efficiently block the chronic

96   inflammation and de novo lipogenesis in HFD mice, and its mechanism might be related to the

97   MAPK/NF-κB and AMPK/SREBP-1c pathways.

98

Materials & Methods

Chemicals and reagents

101   Cyy-287 was synthesized as previously described by our laboratory with a purity over 98%

102   (*Zhang et al., 2022*). Antibodies against p38 (#8690), P-p65 (#3033), P-AMPK (#2535), P-p38

103   (#4511) were purchased from Cell Signaling Technology (Boston, USA). Antibodies against

104   Collagen- Ⅰ (#14695-1-AP) and tubulin (#11224-1-AP) were purchased from Proteintech

105   (Wuhan, China). Anti-SREBP-1c (#abs152294) was obtained from Absin (Shanghai, China).

106   Antibodies for immunohistochemical staining including anti-F4/80 (#ab300421) and anti-TNF-α

107   (#ab183218) were obtained from Abcam (MA, USA). Secondary antibody (#111-585-003) was

108   acquired from Jackson ImmunoResearch (West Grove, USA) and secondary antibody for

109   immunohistochemical staining (#GB23301; #GB23303) were purchased from Servicebio

110   (Wuhan, China). Alanine aminotransferase (ALT) kit (#C009-2-1) and aspartate

111 aminotransferase (AST) kit (#C010-2-1) were obtained from Nanjing Jiancheng Bioengineering

112 Institute (Nanjing, China). Hematoxylin (#G1005), Masson (#G1006) and Sirius red (#G1018)

113 dye solution used for staining of tissue sections were purchased from Servicebio (Wuhan, China).

114 **Animal models**

115 All animal care and experimental procedures were approved on 20-May-2019 by the NIH Guide

116 for the Care and Use of Laboratory Animals approved by the Laboratory Animal Ethics

117 Committee of Wenzhou Medical University for which the Approval ID is WYDW-2019-0809. A

118 total of 36 male C57BL/6J mice weighing 18-22 g were purchased from Vital River Laboratory

119 Animal Center and all were housed in an environmental control room at a temperature of 20 ± 2 ℃

120 and a humidity of $50 \pm 5\%$ with a light/dark cycle of 12 h. During the experimental period, mice

121 had unrestricted access to food and water.

122   Obesity was induced by feeding the mice a high-fat diet (HFD) consisting of 60% fat, 20%

123 protein, and 20% carbohydrate (#D12492) and control mice were fed a standard control diet

124 composed of 10% fat, 20% protein, and 20% carbohydrate. After adaptive feeding for 7 days, the

125 mice were randomly divided into four groups (n ≥ 7): (1) the control group (n = 7); (2) the HFD

126 group (n = 9); (3) the Cyy-287 (5 mg/kg) treated HFD group (n = 10); (4) the Cyy-287 (20

127 mg/kg) treated HFD group (n = 10), according to the principle of random grouping, each animal

128 has an equal chance to be assigned to each experimental group and the control group. After

129 feeding mice with high-fat diet or standard diet for 10 weeks, Cyy-287 was administered daily by

130 gavage at a dose of 5 mg/kg or 20 mg/kg for 10 weeks, mice in control group were given equal

131 volume of normal saline by oral administration. And the body weight was recorded every week.

132 At the 20th week, the blood glucose of mice was recorded with a blood glucose meter.

133 Afterwards, we collected serum samples from mice, followed by collecting liver and heart

134 tissues through gradual CO_2 asphyxiation and cervical dislocation euthanasia.

135 **Measurement of biochemical parameters**

136 A certain weight of liver tissue was weighed, and 9 times of volume of normal saline was added.

137 Under the condition of ice-water bath, mechanical homogenization was performed at 2500 rpm,

138 and centrifugation was performed for 10 min. After the supernatant was further diluted 50 times,

139 ALT and AST enzymes were determined using homologous kits. Taking heparin as

140 anticoagulant, the blood samples were collected and centrifuged at 3,000 rpm at 2-8 ℃ for 15

141 min, and the supernatant was taken, and the serum lipids were detected by automatic biochemical

142   analyzer (Chemray 240).

143   **Echocardiography**

144   The parameters of diastolic function of the heart, such as ejection fraction (EF%) and fractional

145   shortening (FS%), were evaluated by vevo-3100 high-resolution imaging system.

146   **Western blot analysis**

147   Mouse tissues were homogenized in RIPA lysis buffer (#P0013C, Beyotime Biotechnology).

148   Protein contents were measured using BCA assay (#P0012S, Beyotime Biotechnology). The

149   proteins were separated by SDS-PAGE electrophoresis and subsequently electrotransferred to

150   nitrocellulose membranes. After being blocked with a solution of 5% defatted milk in TBST

151   (Tris buffered saline containing 0.05% Tween 20, pH 7.4) for 1.5 h at room temperature, the

152   membranes were incubated with antibodies at 4 ℃ overnight. The membrane was washed three

153   times with TBST solution before being incubated with the secondary antibody. Protein bands

154   were detected by using enhanced chemiluminescence kits. Image J software was used to quantify

155   the intensity of protein bands.

156   **Histological and immunohistochemical (IHC) analyses**

157   Tissue samples were fixed with 10% formalin, embedded in paraffin, sectioned to an 8 μm

158   thickness, stained using hematoxylin and eosin (HE) and Masson's trichrome to assess the extent

159   of tissue fibrosis. In addition, paraffin sections of heart were stained with Sirius Red and paraffin

160   sections of liver were stained with Oil Red to appraise hepatic steatosis. Images were captured

161   using Nikon Eclipse E100 ortho optical microscope (Nikon, Japan). For immunohistochemical

162   experiments, paraffin sections were dewaxed and rehydrated. The tissue was put into citric acid

163   antigen repair buffer for antigen repair, and then put into 3% hydrogen peroxide solution to

164   eliminate endogenous peroxidase. Then the tissue sections were blocked with 3% BSA solution

165   and incubated with anti-TNF-α or F4/80 antibody at 4 ℃ overnight. After incubating with HRP-

166   labeled secondary antibody, the samples were visualized using DAB staining. Images were

167   captured using XSP-C204 biomicroscope (Chongqing chongguang industry co., ltd, China).

168   **Extraction of live microsomes and determination of P450 enzyme content**

169   Add 2.5 mL per gram PBS-Sucrose (0.25 M) buffer to the liver tissue samples and then liver

170   tissue was homogenized. Samples were subsequently centrifuged at 11,000 rpm for 15 min at 4

171   °C. After the supernatant was taken, the centrifugation operation was repeated. Then the samples

172   were centrifuged at 75600 xg in ultracentrifuge for 2 h at 10 °C. The precipitate was resuspended

173   with PBS until the solution was clear. We then determined the CYP450 content in the

174   microsomal samples using the CO differential method. We took 1 mL of microsome samples

175   which were diluted to 1 mg/mL with PBS, aerate with carbon monoxide for 2 min, and then

176   added 5 mg of sodium hydrosulfite. The absorbance at 450 nm and 490 nm was measured by

177   Evolution 201 ultraviolet-visible spectrophotometer (ThermoFisher scientific, USA). The

178   calculation formula is: C (nmol/mL) = (OD 450 nm - OD 490 nm) $*$ 1000 / 91.

179   **Statistical analysis**

180   All data are presented as mean ± standard error of the mean (S.E.M). Statistical significance

181   among groups was determined by Student's t-test for multiple comparisons or one-way analysis

182   of variance (ANOVA). If the variance was uneven, welch correction was used. Differences

183   between groups were considered to be statistically significant when $P < 0.05$ (GraphPad Prism

184   6.0 and SPSS 22.0 softwares).

185

186   # Results

187   **The improvement of Cyy-287 on obesity-induced metabolic disorder**

188   To confirm whether obesity will cause multiple organ damage, especially cardiac and hepatic

189   dysfunction and evaluate the preventive effect of Cyy-287 treatment, we established a high-fat

190   diet (HFD) mice model. After 20 weeks, mice fed with HFD showed a higher rate of weight gain

191   (> 20 g) than mice fed with standard diet (< 5 g), and all their weight exceeded 45 g (**Fig. 1B**).

192   The body mass index (BMI) of HFD mice was significantly increased compared with the control

193   group ($P < 0.0001$), but Cyy-287 treatment could not delay the increasing of BMI (**Fig. 1C**). In

194   addition, the serum glucose level of mice in HFD group increased significantly ($P < 0.001$),

195   indicating the occurrence of hyperglycemia, and Cyy-287 significantly reduced blood glucose

196   compared with HFD group (5 mg/kg, $P < 0.01$; 20 mg/kg, $P < 0.05$; **Fig. 1D**). What's more,

197   Cyy-287 decreased serum lipid markers LDL (5 mg/kg, $P < 0.01$; 20 mg/kg, $P < 0.001$) and TC

198   (5 mg/kg, $P < 0.001$; 20 mg/kg, $P < 0.0001$) in HFD mice (**Fig. 1E** and **2F**). These results

199   showed that Cyy-287 improved the metabolic disorder caused by obesity, including decreased

200   serum glucose and decreased serum lipid production.

201   **The preventive effect of Cyy-287 on obesity-linked cardiac and hepatic**

202   **dysfunction**

203   The mice in the HFD group showed obvious ventricular remodeling characteristics, such as

204   increased ventricular inner diameter and changed ejection fraction (EF, $P < 0.001$) and fractional

205   shortening (FS, $P < 0.001$), confirming the cardiac dysfunction caused by obesity (**Fig. 2A-2C**).

206   Cyy-287 significantly restored mice cardiac function indicators EF (20 mg/kg, $P < 0.001$) and FS

207   (20 mg/kg, $P < 0.001$), and reduced cardiac hypertrophy index in a dose-dependent manner

208   (**Table 1**). The levels of ALT and AST were also significantly increased in the HFD group

209   compared with the control group ($P < 0.0001$), confirming the hepatic dysfunction caused by

210   obesity (**Fig. 2D** and **2E**). Cyy-287 exhibited a remarkably suppressive effect on the elevation of

211   serum ALT (5 mg/kg, $P < 0.001$) and AST (5 or 20 mg/kg, $P < 0.0001$). These outcomes

212   corroborate Cyy-287's efficacy in impeding obesity-related deterioration of cardiac and hepatic

213   functions.

214   **Cyy-287 inhibits obesity-induced cardiac inflammation though suppressing**

215   **MAPK/NF-κB pathway and activating AMPK pathway**

216   To further investigate the effect of Cyy-287 on obesity-induced cardiac dysfunction, we

217   conducted HE and IHC staining. The analysis of the histopathological images showed that HFD

218   caused cardiac morphological changes, including myocardial fiber atrophy and disorder,

219   inflammatory cell infiltration, which were improved after Cyy-287 treatment (**Fig. 3A**). In

220   addition, Cyy-287 treatment reduced the expression of TNF-α in HFD mice. We then evaluated

221   the degree of myocardial fibrosis by Masson and Sirius Red staining in mice. As shown in **Fig.**

222   **3A-3C**, there was significant fibrous proliferation (Masson, $P < 0.001$) and collagen deposition

223   (Sirius Red, $P < 0.05$) in the myocardium of HFD mice, and the progression of myocardial

224   fibrosis was significantly blocked after Cyy-287 treatment (Masson, 20 mg/kg, $P < 0.01$; Sirius

225   Red, 20 mg/kg, $P < 0.05$). Consistent with the results of IHC, western blot results showed that

226   Cyy-287 improved the HFD-induced Collagen- Ⅰ expression (20 mg/kg, $P < 0.05$) (**Fig. 3D**).

227   The HFD group demonstrated markedly elevated levels of phosphorylated p65 (RelA), a crucial

228   subunit of NF-κB, as well as p38, a member of the MAPKs family. Conversely, treatment with

229   Cyy-287 significantly attenuated the cardiac expression of phosphorylated p65 and p38 (20

230   mg/kg, $P < 0.05$), as compared to the HFD-only group. Meanwhile, the phosphorylation of

231   AMPK was greatly inhibited by HFD ($P < 0.05$), and the cardiac expression of phosphorylated

232   AMPK was effectively increased after Cyy-287 treatment ($P = 0.30$). Hence, our findings imply

233 that Cyy-287 proficiently safeguarded the myocardium from harm via the modulation of

234 MAPK/NF-κB and AMPK signaling cascades.

235 Cyy-287 relieves obesity induced liver damage and MAPK/NF-κB pathway protein

236 expression and AMPK activity inhibition

237 Examination of the histopathological illustrations unveiled the morphological alterations brought

238 about by HFD in the liver, comprising hepatic steatosis, inflammatory responses within the

239 hepatic lobules, centrilobular hepatocyte necrosis, and the presence of ballooned hepatocytes

240 (**Fig. 4A**). Cyy-287 undoubtedly alleviated liver damage, and reduced liver cell necrosis and

241 degeneration. In addition, the Masson (20 mg/kg, $P < 0.01$) and F4/80 (20 mg/kg, $P < 0.001$)

242 staining showed that Cyy-287 could reduce hepatic fibrosis and macrophage infiltration

243 compared to the HFD group (**Fig. 4B** and **4C**). Similar to the results in the heart, the

244 phosphorylation of AMPK was greatly inhibited by HFD ($P < 0.05$), and the hepatic expression

245 of phosphorylated AMPK was effectively increased after Cyy-287 treatment (20 mg/kg, $P < 0.05$;

246 **Fig. 4D**). In addition, the hepatic expression of phosphorylated p65 and p38 was effectively

247 decreased after Cyy-287 treatment compared to HFD-only group (20 mg/kg, $P < 0.05$). In

248 conclusion, our histological and western blot analyses substantiate that administering Cyy-287

249 orally thwarted the liver impairment and inflammation triggered by HFD.

250 Cyy-287 relieves obesity induced liver lipid storage and SREBP-1c expression

251 SREBP-1c is a key regulatory transcription factor involved in *de novo* lipogenesis, and the over-

252 expression of SREBP-1c was correlated with the lipid storage in the liver. The Oil Red staining

253 showed that Cyy-287 could reduce fatty accumulation in liver induced by HFD (**Fig. 4A**).

254 Furthermore, the HFD group exhibited a significantly elevated expression level of SREBP-1c

255 compared to the control group ($P < 0.05$; **Fig. 4D**). However, oral administration of Cyy-287

256 effectively curbed the hepatic expression of SREBP-1c in comparison to the HFD-only group

257 (20 mg/kg, $P < 0.05$). Our data categorically establish that the hepatoprotective influence of Cyy-

258 287 owes to its lipid synthesis inhibitory attributes.

259 Cyy-287 restores the content of hepatic CYP450 enzymes

260 As a kind of haemoglobin, cytochrome P450 enzymes (CYP450) participate in the metabolism of

261 many substances, including endogenous substances, exogenous substances, and drugs. CYP450

262 exists mainly in liver microsomes and the activity of CYP450 can be used to evaluate the liver

263 function. Hence, we extracted the mouse liver microsomes and quantify the total amount of

264   CYP450 enzymes. As shown in the **Fig. 5**, the content of hepatic CYP450 enzymes in HFD

265   group mice was significantly reduced ($P < 0.05$), and the reduction of liver CYP450 enzymes

266   content induced by HFD was significantly reversed after Cyy-287 treatment (20 mg/kg; $P <$

267   0.05), which further indicating that Cyy-287 could restore liver function and alleviated the liver

268   injury caused by high fat.

269   **Discussion**

270   Obesity, which has been rising in prevalence worldwide over the past several decades, is now

271   considered a public health epidemic. Studies have found that obese people present a chronic low-

272   grade inflammatory state with imbalance of pro-inflammatory and anti-inflammatory immune

273   cells *(Gregor $ Hotamisligil, 2011)*. Obesity induced inflammation will lead to maladaptive

274   responses such as fibrosis and necrosis that can cause significant tissue damage (*Crewe, An $*

275   *Scherer, 2017*). Moreover, obesity induced inflammation is unique in that it involves multiple

276   organs, including adipose, pancreas, liver, skeletal muscle, heart, and brain. Persistent metabolic

277   inflammation also lead to serious syndrome, including insulin resistance, type 2 diabetes,

278   cardiovascular disease, liver disease, cancer, and neurodegeneration (*Saltiel $ Olefsky, 2017*). It

279   has been reported that anti-inflammatory drugs or natural compounds can alleviate obesity-

280   related metabolic diseases (*Lee et al., 2020; Ngamsamer, Sirivarasai $ Sutjarit, 2022*).

281   Consequently, blocking obesity-induced inflammation could be an effective way to prevent

282   tissue damage and syndrome.

283   Here, we first demonstrated that cyy-287, a novel pyrimidine-2,4-diamine derivative, had

284   a strong inhibitory effect on HFD induced inflammation and tissue injury. The NF-κB pathway is

285   a critical signaling axis mediating the expression of inflammation-related mediators such as via

286   NF-κB-binding motifs in their promoters (*Dorrington $ Fraser, 2019*). NF-κB protein is mainly

287   composed of two subunits, p50 and p65, which could be activated by cytokines, pathogens, and

288   radiation (*Liu , Zhang $ Joo, 2017*). In this study, we found that Cyy-287 can significantly inhibit

289   NF-κB p65-mediated inflammatory pathway in heart and liver tissues of obese mice. Oral

290   administration of Cyy-287 to HFD mice induced a noteworthy decline in the histopathological

291   disruption of the heart and liver, characterized by attenuation in macrophage infiltration, fibrosis,

292   and necrotic deterioration. Furthermore, Cyy-287 enhanced EF and FS and reduced the serum

293   AST and ALT levels that ensue due to liver functional impairment induced by HFD.

294   Additionally, Cyy-287 effectively curbed abnormal hepatic lipid aggregation (TG). Thus, our

295   data support the idea that Cyy-287 could effectively protect against the obesity-induced cardiac

296   and hepatic damage via inhibiting the NF-κB mediated inflammatory pathway.

297   As a fundamental transducer of upstream signaling for NF-κB, the MAPKs family is

298   intricately linked to cell death and is accountable for generating proinflammatory cytokines.

299   Several studies have shown that MAPK is involved in oxidative stress and apoptosis, and

300   blocking MAPK signaling pathway can prevent paracetamol-induced hepatotoxicity by

301   regulating pro-inflammatory cytokines (*Noh et al., 2013*). In addition, research suggested that

302   curcumin reduces chemical and drug-induced cardiotoxicity by inhibiting p38 MAPK signaling

303   pathway (*Yarmohammadi, Hayes $ Karimi, 2021*). Our western blot data showed that HFD

304   activated the expression of P-p38, leading to cardiomyocyte and hepatocyte injury. Cyy-287

305   effectively protected the heart and liver from damage by inhibiting the MAPK pathway.

306   As a highly conserved regulator of metabolism, AMPK is also a critical component in the

307   prevention of various inflammatory signaling pathways, which may represent a larger therapeutic

308   target for the control of insulin resistance, diabetes, and obesity (*Noor et al., 2020*). A recent

309   study showed that the CaMKKβ/LKB1/AMPK axis and Ca2+ levels can provide a quick,

310   adaptable switch to promote cell survival (*Yang et al., 2020*). In addition, activation of AMPK

311   alleviates paracetamol-induced hepatotoxicity by inhibiting the release of pro-inflammatory

312   cytokines and abnormal lipid metabolism (*Jiang et al., 2021*). In recent years, cardiomyopathy

313   caused by obesity has attracted more and more attention. Studies have shown that upregulating

314   the SIRT1/LKB1/AMPK pathway can reduce obesity-induced cardiomyopathy (*Li et al., 2022*).

315   Our findings evinced that the elevation in the phosphorylation of AMPK was elicited by the

316   administration of Cyy-287. Additionally, our results highlighted that the administration of Cyy-

317   287 repressed obesity-related cardiac and hepatic injury by upregulating the AMPK signaling

318   pathway.

319   It is reported that the accumulation of liver fat will lead to inflammation and further liver

320   damage. SREBP-1c is an important transcription factor in de novo lipogenesis and play a key

321   role in regulating liver fat metabolism. The entry of SREBP-1c into the nucleus is regulated by

322   AMPK (*Chao et al.2019*). The western blot results showed that Cyy-287 could regulate AMPK-

323   SREBP-1c signal pathway to improve metabolic disorders caused by HFD in liver. Oil Red

324   staining results further confirmed that Cyy-287 alleviated the excessive accumulation of liver fat.

325   In addition, the levels of lipid markers (LDL and TC) in HFD mice were decreased after Cyy-

326 287 treatment. Thus, our data suggested that Cyy-287 can effectively reduce liver lipid synthesis
327 and fat accumulation in HFD mice by inhibiting SREBP-1c.

328   Unfortunately, our research still has some limitations. In this study, the specific
329 mechanism of Cyy-287 changing AMPK activity has not been clarified, and the molecular
330 mechanism has not been deeply studied. We will do further research in the follow-up study.

Conclusions

332 In this paper, we provided evidence that Cyy-287 has a significant therapeutic effect on obesity-
333 induced heart and liver damage by inhibiting inflammatory response and lipogenesis in HFD
334 mice. The mechanisms of action were revealed to involve Cyy-287's potent anti-inflammatory
335 properties, mediated by inhibiting the NF-κB and MAPK signaling pathways; activating AMPK
336 signalling pathways; and suppressing liver lipid synthesis (**Fig. 6**). Therefore, Cyy-287 has the
337 potential to be a therapeutic drug to reduce the complications of obesity.

338

Acknowledgements

340 The authors declare that they have no conflict of interest.

341

Funding statement:

343 This work was supported by the grants from the Wenzhou Municipal Science and Technology
344 Bureau (No. 2020Y1214), the Natural Science Foundation of Zhejiang Province (No.
345 LQ21H310007), and the National Natural Science Foundation of China (Nos. 82203839 and
346 81973168).

347

References

349 **Aron-Wisnewsky J, Warmbrunn MV, Nieuwdorp M, Clément K. 2020.** Metabolism and
350   Metabolic Disorders and the Microbiome: The Intestinal Microbiota Associated With
351   Obesity, Lipid Metabolism, and Metabolic Health-Pathophysiology and Therapeutic
352   Strategies. *Gastroenterology* **160(2)**:573-599 DOI 10.1053/j.gastro.2020.10.057.
353 **Caballero B. 2019.** Humans against Obesity: Who Will Win? *Advances in Nutrition*
354   **10(suppl_1)**:S4-S9 DOI 10.1093/advances/nmy055.

355 **Chao HW, Chao SW, Lin H, Ku HC, Cheng CF. 2019.** Homeostasis of Glucose and Lipid in

356   Non-Alcoholic Fatty Liver Disease. *International Journal of Molecular Sciences* **20(2)**: 298

357   DOI 10.3390/ijms20020298.

358 **Cox AJ, West NP and Cripps AW. 2015.** Obesity, inflammation, and the gut microbiota. *The*

359   *Lancet Diabetes and Endocrinology* **3(3)**:207-15 DOI 10.1016/S2213-8587(14)70134-2.

360 **Crewe C, An YA, Scherer PE. 2017.** The ominous triad of adipose tissue dysfunction:

361   inflammation, fibrosis, and impaired angiogenesis. *Journal Of Clinical Investigation*

362   127(1):74-82 DOI 10.1172/JCI88883.

363 **Dorrington MG, Fraser IDC. 2019.** NF-κB Signaling in Macrophages: Dynamics, Crosstalk,

364   and Signal Integration. *Frontiers in Immunology* **10**:705 DOI 10.3389/fimmu.2019.00705.

365 **Fogarty S, Ross FA, Vara Ciruelos D, Gray A, Gowans GJ, Hardie DG. 2016.** AMPK causes

366   cell cycle arrest in LKB1-deficient cells via activation of CAMKK2. *Molecular Cancer*

367   *Research* **14(8)**:683-695 DOI 10.1158/1541-7786.

368 **Fu S, Yang L, Li P, Hofmann O, Dicker L, Hide W, Lin X, Watkins SM, Ivanov AR,**

369   **Hotamisligil GS. 2011.** Aberrant lipid metabolism disrupts calcium homeostasis causing

370   liver endoplasmic reticulum stress in obesity. *Nature* 473(7348):528-31

371   DOI 10.1038/nature09968.

372 **Garcia D, Hellberg K, Chaix A, Wallace M, Herzig S, Badur MG, Lin T, Shokhirev MN,**

373   **Pinto AFM, Ross DS, Saghatelian A, Panda S, Dow LE, Metallo CM, Shaw RJ. 2019.**

374   Genetic Liver-Specific AMPK Activation Protects against Diet-Induced Obesity and

375   NAFLD. *Cell Reports* **26(1)**:192-208 DOI 10.1016/j.celrep.2018.12.036.

376 **Goldman S, Zhang Y, Jin S. 2010.** Autophagy and adipogenesis: implications in obesity and

377   type II diabetes. *Autophagy* **6(1)**:179-81 DOI 10.4161/auto.6.1.10814.

378 **Gregor MF, Hotamisligil GS. 2011.** Inflammatory mechanisms in obesity. *Annual Review of*

379   *Immunology* **29**:415-445 DOI 10.1146/annurev-immunol-031210-101322.

380 **Jackson VM, Breen DM, Fortin JP, Liou A, Kuzmiski JB, Loomis AK, Rives ML, Shah B,**

381   **Carpino PA. 2015.** Latest approaches for the treatment of obesity. *Expert Opinion on Drug*

382   *Discovery* **10(8)**:825-39 DOI 10.1517/17460441.2015.1044966.

383 **Klop B, Elte JW, Cabezas MC. 2013.** Dyslipidemia in obesity: mechanisms and potential

384   targets. *Nutrients* **5(4)**:1218-40 DOI 10.3390/nu5041218.

385 **Lee ES, Kwon MH, Kim HM, Woo HB, Ahn CM, Chung CH. 2019.** Curcumin analog

386   CUR5-8 ameliorates nonalcoholic fatty liver disease in mice with high-fat diet-induced

387   obesity. *Metabolism* **103**:154015 DOI 10.1016/j.metabol.2019.154015.

388 **Li SN, Yu YL, Wang BY, Qiao SY, Hu MM, Wang H, Fu CN, Dong B. 2022.**

389   Overexpression of G Protein-Coupled Receptor 40 Protects Obesity-Induced

390   Cardiomyopathy Through the SIRT1/LKB1/AMPK Pathway. *Human Gene Therapy* **33(11-**

391   **12)**:598-613 DOI 10.1089/hum.2021.176.

392 **Li YC, Qiao JY, Wang BY, Bai M, Shen JD, Cheng YX. 2018.** Paeoniflorin ameliorates

393   fructose-induced insulin resistance and hepatic steatosis by activating LKB1/AMPK and

394   AKT pathways. *Nutrients* **10(8)**:1024 DOI 10.3390/nu10081024.

395 **Li YC, Qiao JY, Wang BY, Bai M, Shen JD, Cheng YX. 2021.** Sanghuangporus sanghuang

396   Mycelium Prevents Paracetamol-Induced Hepatotoxicity through Regulating the

397   MAPK/NF-κB, Keap1/Nrf2/HO-1, TLR4/PI3K/Akt, and CaMKKβ/LKB1/AMPK Pathways

398   and Suppressing Oxidative Stress and Inflammation. *Antioxidants* **10(8)**:897

399   DOI 10.3390/antiox10060897.

400 **Li Z, Li J, Miao X, Cui W, Miao L, Cai L. 2021.** A minireview: Role of AMP-activated

401   protein kinase (AMPK) signaling in obesity-related renal injury. *Life Science* **265**:118828

402   DOI 10.1016/j.lfs.2020.118828.

403 **Liu T, Zhang L, Joo D. 2017.** NF-κB signaling in inflammation. *Signal Transduction And*

404   *Targeted Therapy* **2**:17023 DOI 10.1038/sigtrans.2017.23.

405 **Lv H, Hong L, Tian Y, Yin C, Zhu C, Feng H. 2019.** Corilagin alleviates acetaminophen-

406   induced hepatotoxicity via enhancing the AMPK/GSK3beta-Nrf2 signaling pathway. *Cell*

407   *Communication And Signaling* **17(1)**:2 DOI 10.1186/s12964-018-0314-2.

408 **Narayanaswami V, Dwoskin LP. 2017.** Obesity: Current and potential pharmacotherapeutics

409   and targets. *Pharmacology and Therapeutics* **170**: 116-147

410   DOI org/10.1016/j.pharmthera.2016.10.015.

411 **Ngamsamer C, Sirivarasai J, Sutjarit N. 2022.** The Benefits of Anthocyanins against Obesity-

412   Induced Inflammation. *Biomolecules* **12(6)**:852 DOI 10.3390/biom12060852.

413 **Nguyen NU, Stamper BD. 2017.** Polyphenols reported to shift paracetamol-induced changes in

414   MAPK signaling and toxicity outcomes. *Chemico-Biological Interactions* **277**:129-136

415   DOI 10.1016/j.cbi.2017.09.007.

416 **Noh JR, Kim YH, Hwang JH, Gang GT, Kim KS, Lee IK, Yun BS, Lee CH. 2013.**

417   Davallialactone protects against acetaminophen overdose-induced liver injuries in mice.

418   *Food and Chemical Toxicology* **58**:14-21 DOI 10.1016/j.fct.2013.04.005.

419 **Noor HB, Mou NA, Salem L, Shimul MFA, Biswas S, Akther R, Khan S, Raihan S, Mohib**

420   **MM, Sagor MAT. 2020.** Anti-inflammatory Property of AMP-activated Protein Kinase.

421   *Anti-Inflammatory & Anti-Allergy Agents in Medicinal Chemistry* **19(1)**: 2-41

422   DOI 10.2174/1871523018666190830100022.

423 **Piche ME, Tchernof A, Despres JP. 2020.** Obesity Phenotypes, Diabetes, and Cardiovascular

424   Diseases. *Circulation Research* **126(11)**:1477-1500

425   DOI 10.1161/CIRCRESAHA.120.316101.

426 **Polyzos SA, Kountouras J, Mantzoros CS. 2019.** Obesity and nonalcoholic fatty liver disease:

427   From pathophysiology to therapeutics. *Metabolism* **92**:82-97

428   DOI 10.1016/j.metabol.2018.11.014.

429 **Saltiel AR, Olefsky JM. 2017.** Inflammatory mechanisms linking obesity and metabolic disease.

430   *Journal Of Clinical Investigation* **127(1)**:1-4 DOI 10.1172/JCI92035.

431 **Sang T, Guo C, Guo D, Wu J, Wang Y, Wang Y, Chen J, Chen C, Wu K, Na K, Li K, Fang**

432   **L, Guo C, Wang X. 2021.** Suppression of obesity and inflammation by polysaccharide from

433   sporoderm-broken spore of Ganoderma lucidum via gut microbiota regulation.

434   *Carbohydrate Polymers* **256**:117594 DOI 10.1016/j.carbpol.2020.117594.

435 **Srivastava G, Apovian CM. 2017.** Current pharmacotherapy for obesity. *Nature Reviews*

436   *Endocrinology* **14(1)**:12-24 DOI 10.1038/nrendo.2017.122.

437 **Tanaka M. 2020.** Improving obesity and blood pressure. *Hypertension Research* **43(2)**:79-89

438   DOI 10.1038/s41440-019-0348-x.

439 **Wu Y, Shi T, Wang J, He R. 2021.** Talabostat Alleviates Obesity and Associated Metabolic

440   Dysfunction via Suppression of Macrophage-Driven Adipose Inflammation. *Obesity*

441   **29(2)**:327-336 DOI 10.1002/oby.23058.

442 **Yang R, Song C, Chen J, Zhou L, Jiang X, Cao X, Sun Y, Zhang Q. 2020.** Limonin

443   ameliorates acetaminophen-induced hepatotoxicity by activating Nrf2 antioxidative pathway

444   and inhibiting NF-κB inflammatory response via upregulating Sirt1. *Phytomedicine*

445   **69**:153211 DOI 10.1016/j.phymed.2020.153211.

446   **Yarmohammadi F, Hayes AW, Karimi G. 2021.** Protective effects of curcumin on chemical

447   and drug-induced cardiotoxicity: a review. *Naunyn-Schmiedeberg's Archives of*

448   *Pharmacology* **394(7)**:1341-1353 DOI 10.1007/s00210-021-02072-8.

449   **Ye J. 2021.** Mechanism of insulin resistance in obesity: a role of ATP. *Frontiers of Medicine*

450   **15(3)**:372-382 DOI 10.1007/s11684-021-0862-5

451   **Zhang Q, Huang H, Zheng S, Tang Y, Zhang X, Zhu Q, Ni Z, Zheng X, Wang K, Huang L,**

452   **Zhao Y, Liu Z, Qian J. 2022.** cyy-287, a novel pyrimidine-2,4-diamine derivative, inhibits

453   tumor growth of EGFR-driven non-small cell lung cancer via the ERK pathway. *Acta*

454   *Biochimica et Biophysica Sinica* **54(10)**:1540-1551 DOI 10.3724/abbs.2022139.

455 **Figure legends**

456 **Figure1. Cyy-287 restrains the occur of hyperglycosemia and hyperlipidemia**

457 **induced by HFD in mice.** (A) The chemical structure of cyy-287. (B) Body weight changes

458 in mice. (C) The BMI of mice (n≥7). The serum glucose level (n≥7) (D), lipid markers LDL

459 (n=3) (E) and TC (n=3) (F) of mice treated under different conditions was measured. Data are

460 presented as the mean $\pm$ SEM. *** $P < 0.001$, **** $P < 0.0001$ compared with the control group.

461 $^{\#}P < 0.05$, $^{\#\#}P < 0.01$, $^{\#\#\#}P < 0.001$, $^{\#\#\#\#}P < 0.0001$ compared with the HFD group.

462

463 **Figure2. Cyy-287 improves cardiac and hepatic dysfunction induced by HFD in**

464 **mice.** (A) Representative mechocardiography M-mode images in mice. (B and C)

465 Quantification of cardiac function indexes (n=5). (D and E) Determination of AST and ALT

466 (n≥6). Data are presented as the mean $\pm$ SEM. *** $P < 0.001$, **** $P < 0.0001$ compared with

467 the control group. $^{\#\#\#}P < 0.001$, $^{\#\#\#\#}P < 0.0001$ compared with the HFD group.

468

469 **Figure3. Cyy-287 attenuates myocardial inflammation and fibrosis by inhibiting**

470 **p38 MAPK and activating AMPK in HFD mice.** (A) Tissue sections were analysed by HE,

471 Masson, and Sirus Red and IHC using anti-TNF-α antibody (scale bar: 50 μm). (B and C)

472 Quantitative data of Masson and Sirus Red staining in (A). (D) Proteins were extracted from

473 myocardium and then subject to western blot analysis. Quantified results were plotted. Data are

474 presented as the mean $\pm$ SEM (n=3). $*P < 0.05$, *** $P < 0.001$ compared with the control group.

475 $^{\#}P < 0.05$, $^{\#\#}P < 0.01$ compared with the HFD group.

476

477 **Figrue4. Cyy-287 mitigates hepatic fat accumulation and damage though p38**

478 **MAPK/NF-κB dowregulation and activating AMPK in HFD mice.** (A) Tissue sections

479 were analysed by HE, Oil Red, and Masson and IHC using F4/80 anti-body (scale bar: 50 μm).

480 (B and C) Quantitative data of Masson and F4/80 in (A). (D) Proteins were extracted from

481 myocardium and then subject to western blot analysis. Quantified results were plotted. Data are

482 presented as the mean $\pm$ SEM (n=3). $*P < 0.05$, **** $P < 0.001$ compared with the control

483 group. $^{\#}P < 0.05$, $^{\#\#}P < 0.01$, $^{\#\#\#}P < 0.001$ compared with the HFD group.

484

485 **Figure5. Cyy-287 increases the content of CYP450 enzymes in liver microsomes**

486 **of HFD mice.** (A) Representative UV chromatograms of liver microsomes. (B) Quantification

487 of liver microsomal content. Data are presented as the mean $\pm$ SEM (n=3). $*P < 0.05$ compared

488 with the control group. $^{\#}P < 0.05$ compared with the HFD group.

489

490 **Figure6. The mechanism for the protective effect of Cyy-287 on HFD-induced**

491 **inflammation.**

492

493 **Table 1. Echocardiographic parameters of rats (n≥5).**

Figure 1

Figure1. Cyy-287 restrains the occur of hyperglycosemia and hyperlipidemia induced by HFD in mice.
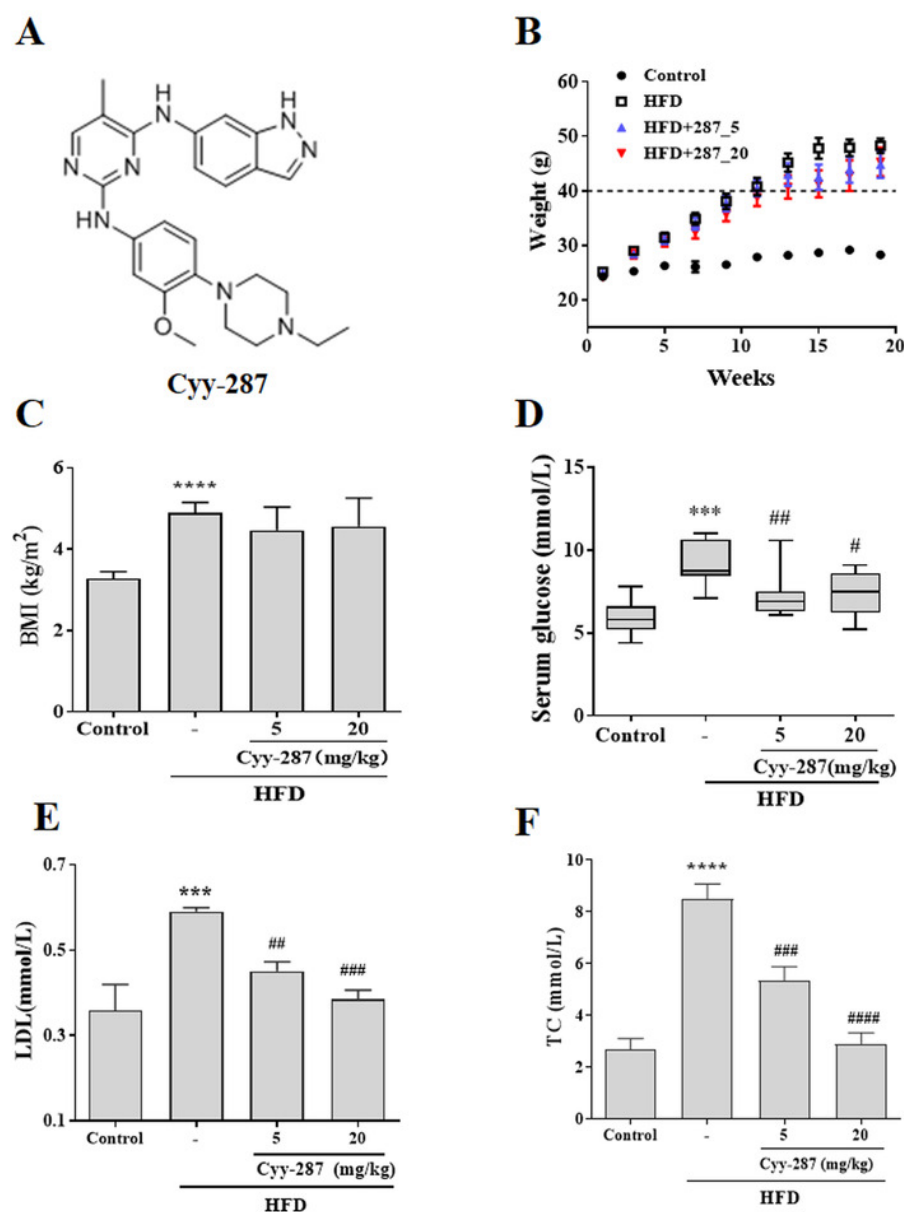
Figure 2

Figure2. Cyy-287 improves cardiac and hepatic dysfunction induced by HFD in mice.
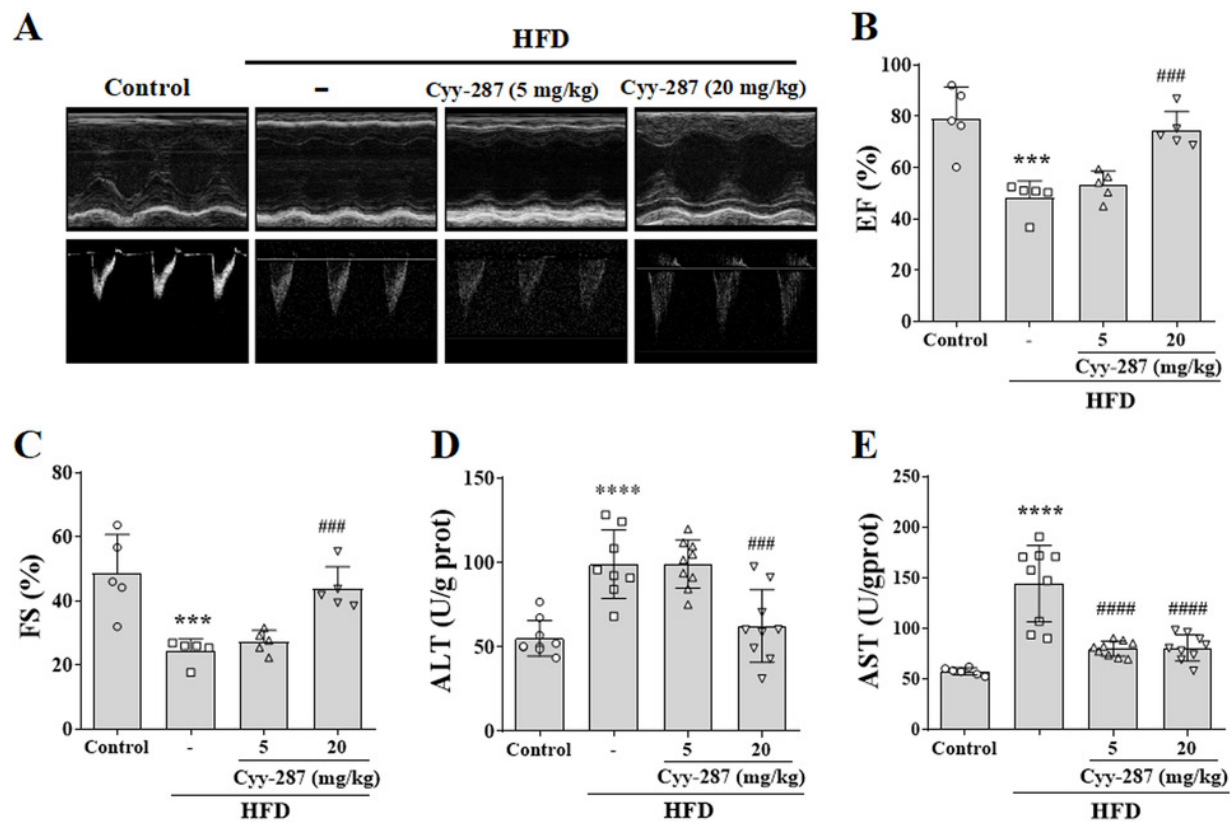
Figure2

Figure 3

Figure3. Cyy-287 attenuates myocardial inflammation and fibrosis by inhibiting p38 MAPK and activating AMPK in HFD mice.

Figure3
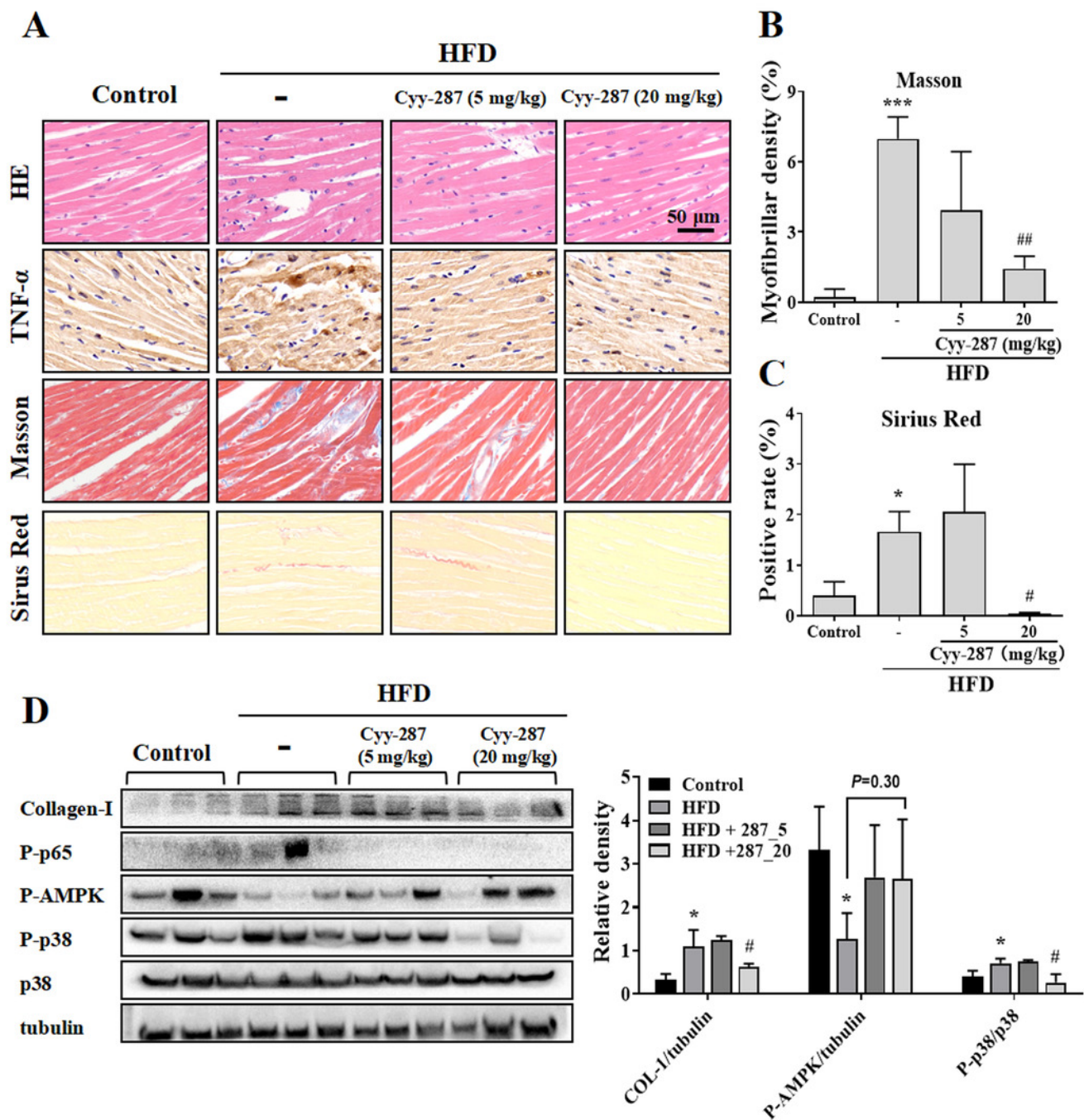
Figure 4

Figrue4. Cyy-287 mitigates hepatic fat accumulation and damage though p38 MAPK/NF-κB dowregulation and activating AMPK in HFD mice.

Figure4

A

HFD

Control | - | Cyy-287 (5 mg/kg) | Cyy-287 (20 mg/kg)

HE
Masson
F4/80
Oil Red

50 μm

B

Masson

C

F4/80

D

HFD

Control | - | Cyy-287 (5 mg/kg) | Cyy-287 (20 mg/kg)

Collagen-I
P-AMPK
P-p65
P-p38
p38
SREBP-1c
tubulin

Control
HFD
HFD + 287_5
HFD + 287_20

Relative density

P-AMPK/tubulin P-p65/tubulin P-p38/p38 SREBP-1c/tubulin
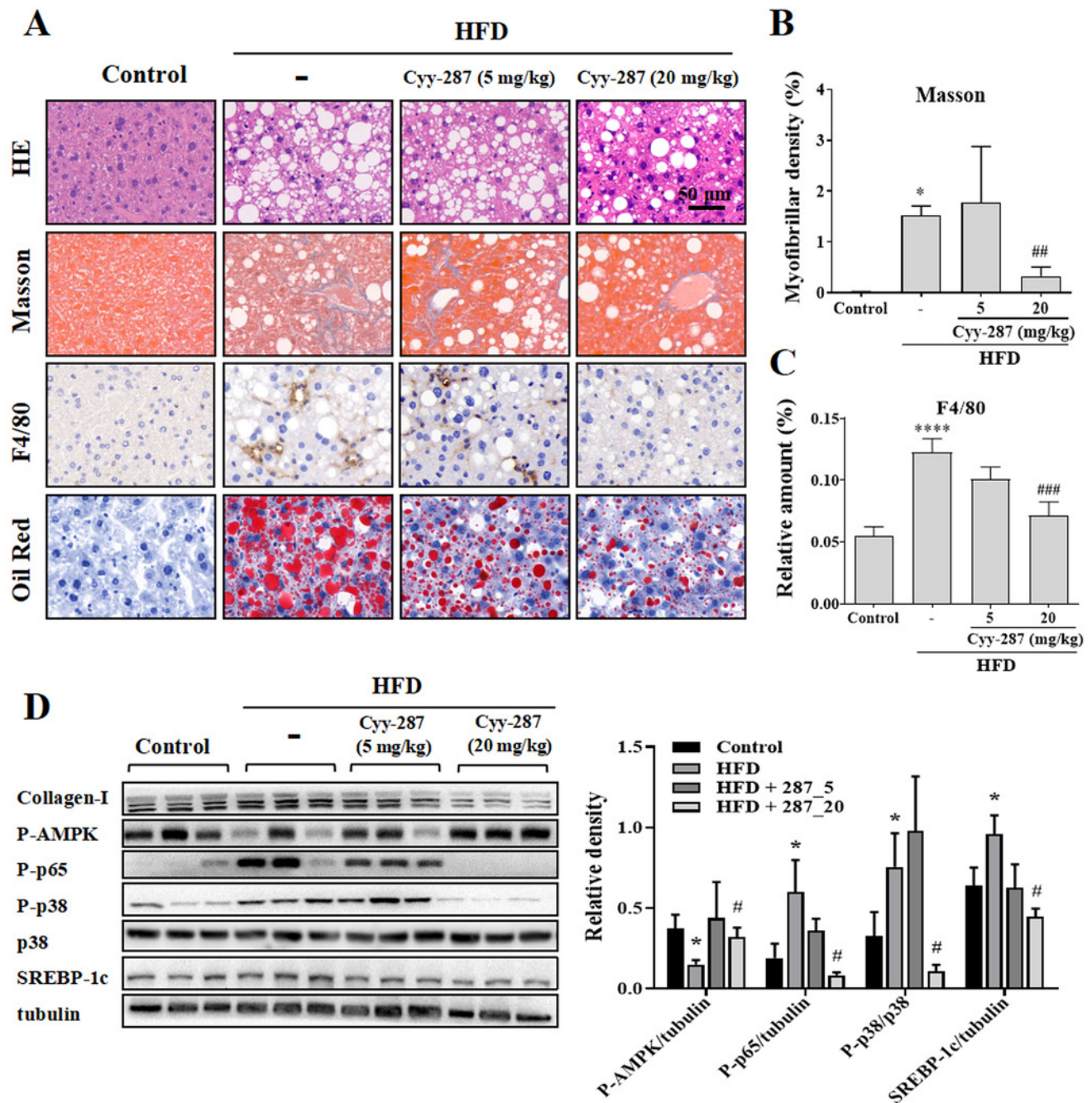
Figure 5

Figure5. Cyy-287 increases the content of CYP450 enzymes in liver microsomes of HFD mice.

Figure5

A

Control

HFD

HFD+Cyy-287 (5mg/kg)

HFD+Cyy-287 (20mg/kg)

B
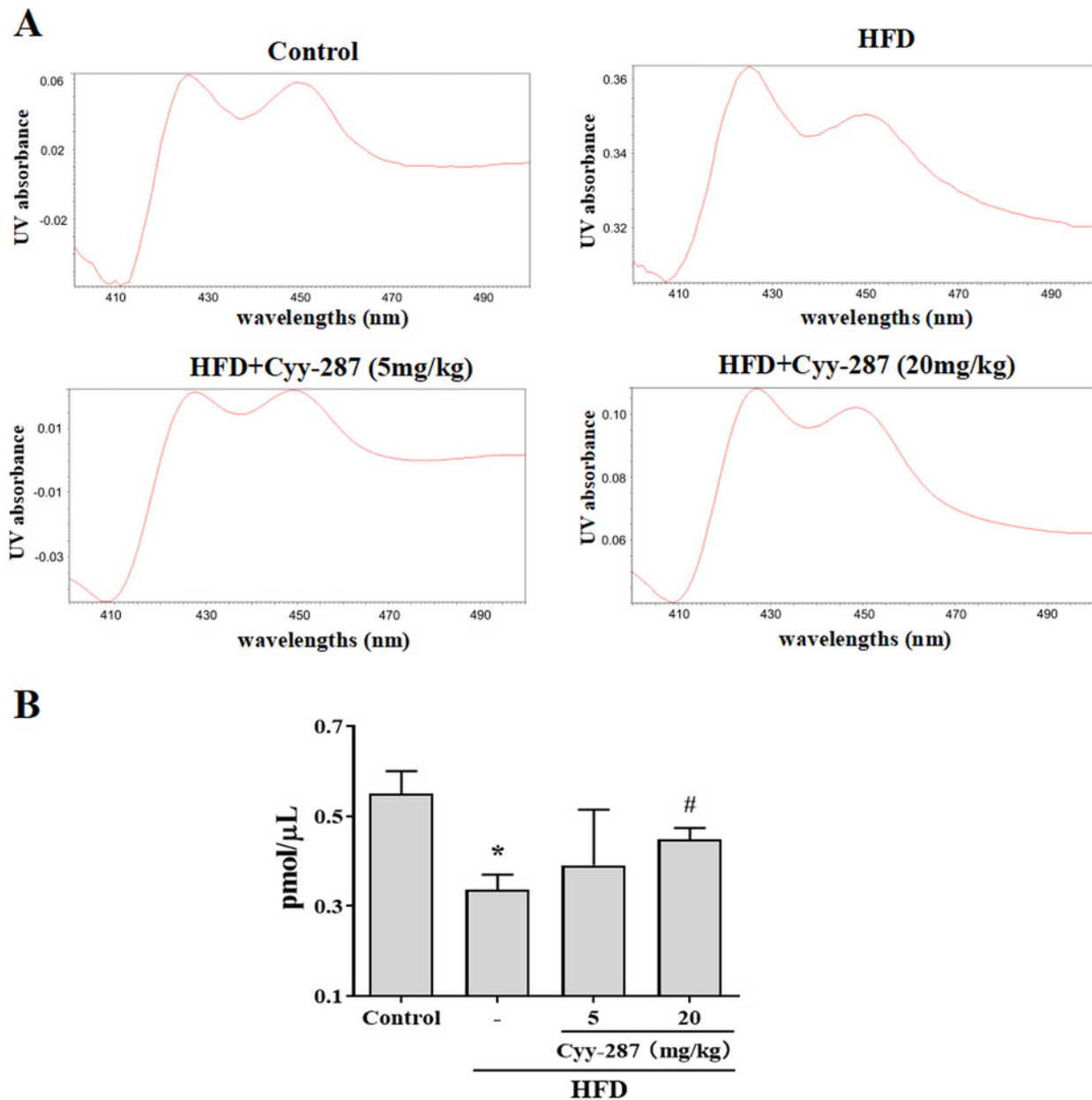
Figure 6

Figure6. The mechanism for the protective effect of Cyy-287 on HFD-induced inflammation.

Figure6
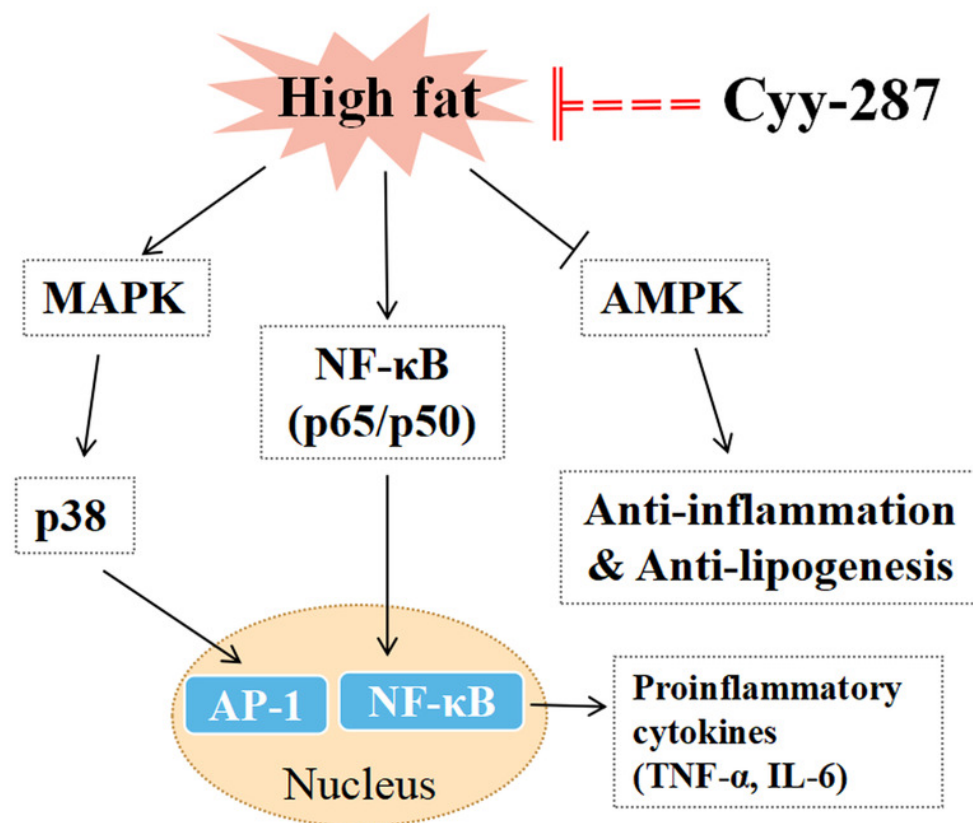
Table 1. Echocardiographic parameters of rats (n≥5).

1   Table 1. Echocardiographic parameters of rats (n≥5).

Parameter	Units	Control	HFD	Cyy-287 (5mg/kg)	Cyy-287 (20mg/kg)
Diameter;d (LV Trace)	mm	3.7±0.48	4.55±0.26*	4.4±0.36	4.16±0.44
Diameter;s (LV Trace)	mm	1.94±0.69	3.44±0.31***	3.2±0.31	2.36±0.48#
EF (LV Trace)	%	78.98±12.38	48.31±6.56***	53.12±5.58	74.74±7.15###
FS (LV Trace)	%	48.51±12.2	24.34±3.8***	27.26±3.55	43.77±6.85##
V;d (LV Trace)	uL	59.58±19.02	95.2±12.77*	88.58±16.89	77.86±18.31
V;s (LV Trace)	uL	14.03±12.92	49.48±11.01***	41.58±9.66	20.53±8.55##

(EF, Ejection fraction; FS, Fractional shortening; V;d, Left ventricular diastolic volume; V;s, Left ventricular systolic volume. $* P < 0.05$, $*** P < 0.001$ compared with the control group. $^{\#} P < 0.05$, $^{\#\#} P < 0.01$, $^{\#\#\#} P < 0.001$ compared with the HFD group.)